



POLITECNICO
MILANO 1863

SCUOLA DI INGEGNERIA INDUSTRIALE
E DELL'INFORMAZIONE
SCUOLA DI INGEGNERIA CIVILE,
AMBIENTALE E TERRITORIALE



EXECUTIVE SUMMARY OF THE THESIS

Stabilized and self-stabilized virtual elements based on the Hu-Washizu variational principle for 3D linear elastostatics

DOUBLE DEGREE MASTER THESIS IN CIVIL ENGINEERING - MATHEMATICAL ENGINEERING

Author: ELIAS PESCIALLI

Advisor: PROF. MASSIMILIANO CREMONESI

Co-advisor: PROF. UMBERTO PEREGO

Academic year: 2022-2023

Introduction

This work focuses on a numerical partial differential equation solver named *Virtual Element Method* (VEM, [2]), which allows to use general, possibly non-convex polygons/polyhedra and even elements with curved boundaries, support the embedding of hanging nodes and can easily be integrated in standard FEM environments. The key idea, already implemented in generalized/extended finite element methods, relies on the addition of suitable *non-polynomial* functions to the usual finite element spaces. The novelty of the VEM, however, consists in performing a particular choice of the spaces and the degrees of freedom so that computing the stiffness matrix does not require the computation of the non-polynomial shape functions, whose explicit expressions are actually never needed throughout the scheme. It is then possible to deal with complicated element geometries and higher-order continuity requirements, making the method applicable to a wide range of problems and variants.

In this particular work, a version of the VEM for 3D linear elastostatics is presented, developed from a mixed variational formulation based on the three-field Hu-Washizu functional.

Moreover, improvements of standard VEM are sought to address two major drawbacks: (1) the cumbersome projection operation over the faces of each element of the virtual shape functions onto the space of polynomials and (2) the need of stabilization for the local stiffness matrix which exhibits a surplus of rank deficiency. Very few works are available concerning this second issue, solving it only for 2D VEM ([3]).

This thesis proposes the adoption of polyhedral elements with only triangular faces (*delta-hedra*, hence Δ VEM) and modifies their first order formulation ($k = 1$ Δ VEM) by carefully enhancing the strain field. It is shown how a local linear strain model is not sufficient to achieve self-stabilization while three non-complete quadratic polynomial strain fields are proposed and successfully tested for 8-nodes 24-DOFs self-stabilizing virtual elements.

1. Hu-Washizu variational formulation

In this work the VEM scheme is constructed starting from a very general mixed finite element formulation which exploits the Hu-Washizu variational principle: the action of the Hu-Washizu

functional (1) is stationary.

$$\begin{aligned} \Pi(\mathbf{u}, \boldsymbol{\varepsilon}, \boldsymbol{\sigma}) = & \frac{1}{2} \int_{\Omega} \boldsymbol{\varepsilon}^T \mathbf{D} \boldsymbol{\varepsilon} d\Omega + \\ & - \int_{\Omega} \boldsymbol{\sigma}^T (\boldsymbol{\varepsilon} - \mathbf{S} \mathbf{u}) d\Omega + \\ & - \int_{\Omega} \mathbf{u}^T \mathbf{b} d\Omega - \int_{\partial_p \Omega} \mathbf{u}^T \mathbf{p} d\Sigma \quad (1) \end{aligned}$$

where \mathbf{u} , $\boldsymbol{\varepsilon}$ and $\boldsymbol{\sigma}$ are the Voigt vectors of the displacement, strain and stress field respectively, \mathbf{S} the symmetric gradient operator in matrix form, \mathbf{b} the body forces, \mathbf{p} the surface tractions and \mathbf{D} the material elastic stiffness matrix of the body Ω depicted in Figure 1.

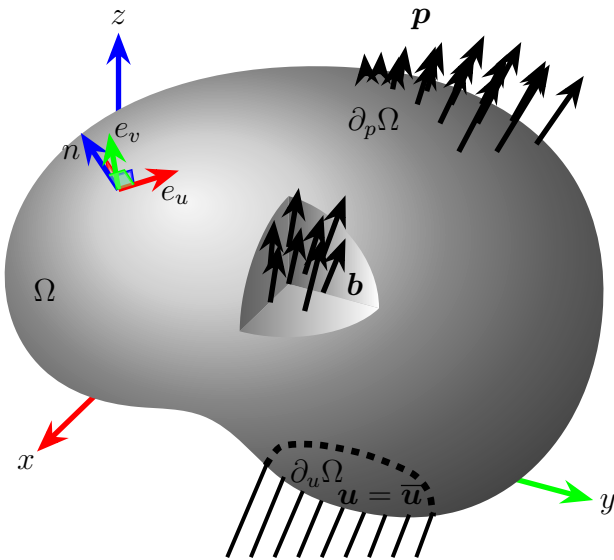


Figure 1: Elastic boundary value problem.

Introducing in the local version of (1), Π_e , the approximations for the three local fields

$$\mathbf{u}(\boldsymbol{\xi}) \approx \mathbf{u}^h(\boldsymbol{\xi}) = \mathbf{N}_u(\boldsymbol{\xi}) \hat{\mathbf{u}} \quad (2)$$

$$\boldsymbol{\varepsilon}(\boldsymbol{\xi}) \approx \boldsymbol{\varepsilon}^h(\boldsymbol{\xi}) = \mathbf{N}_\varepsilon(\boldsymbol{\xi}) \hat{\boldsymbol{\varepsilon}} \quad (3)$$

$$\boldsymbol{\sigma}(\boldsymbol{\xi}) \approx \boldsymbol{\sigma}^h(\boldsymbol{\xi}) = \mathbf{N}_\sigma(\boldsymbol{\xi}) \hat{\boldsymbol{\sigma}} \quad (4)$$

as a function of the non-dimensional barycentric local coordinate $\boldsymbol{\xi}$

$$\boldsymbol{\xi} = \frac{\mathbf{x} - \mathbf{x}_G}{h_e} \quad (5)$$

with \mathbf{x}_G the centroid of the element and h_e its diameter, the discretized local functional be-

comes

$$\begin{aligned} \Pi_e^h(\hat{\mathbf{u}}, \hat{\boldsymbol{\varepsilon}}, \hat{\boldsymbol{\sigma}}) = & \frac{1}{2} \hat{\boldsymbol{\varepsilon}}^T \left(\int_{\Omega_e} \mathbf{N}_\varepsilon^T \mathbf{D} \mathbf{N}_\varepsilon d\Omega \right) \hat{\boldsymbol{\varepsilon}} + \\ & - \hat{\boldsymbol{\sigma}}^T \left(\int_{\Omega_e} \mathbf{N}_\sigma^T (\mathbf{N}_\varepsilon \hat{\boldsymbol{\varepsilon}} - \mathbf{S} \mathbf{N}_u \hat{\mathbf{u}}) d\Omega \right) + \\ & - \hat{\mathbf{u}}^T \left(\int_{\Omega_e} \mathbf{N}_u^T \mathbf{b} d\Omega + \int_{\partial_p \Omega_e} \mathbf{N}_u^T \mathbf{p} d\Sigma \right) \quad (6) \end{aligned}$$

Since $\hat{\boldsymbol{\sigma}}$ and $\hat{\boldsymbol{\varepsilon}}$ are generalized variables, it follows

$$\int_{\Omega_e} \mathbf{N}_\sigma^T \mathbf{N}_\varepsilon d\Omega = \mathbf{I} \quad (7)$$

and the choice for \mathbf{N}_σ satisfying (7)

$$\mathbf{N}_\sigma = \mathbf{N}_\varepsilon \left(\int_{\Omega_e} \mathbf{N}_\varepsilon^T \mathbf{N}_\varepsilon d\Omega \right)^{-1} = \mathbf{N}_\varepsilon \mathbf{G}^{-1} \quad (8)$$

leads to

$$\begin{aligned} \Pi_e^h(\hat{\mathbf{u}}, \hat{\boldsymbol{\varepsilon}}, \hat{\boldsymbol{\sigma}}) = & \frac{1}{2} \hat{\boldsymbol{\varepsilon}}^T \mathbf{E} \hat{\boldsymbol{\varepsilon}} - \hat{\boldsymbol{\sigma}}^T (\hat{\boldsymbol{\varepsilon}} - \mathbf{C} \hat{\mathbf{u}}) + \\ & - \hat{\mathbf{u}}^T \mathbf{F}_e \quad (9) \end{aligned}$$

where the elastic matrix \mathbf{E} and the local equivalent nodal forces vector \mathbf{F}_e are clear from (6), and the compatibility matrix \mathbf{C} is

$$\begin{aligned} \mathbf{C} = & \int_{\Omega_e} \mathbf{N}_\sigma^T \mathbf{S} \mathbf{N}_u d\Omega = \\ = & \mathbf{G}^{-1} \int_{\Omega_e} \mathbf{N}_\varepsilon^T \mathbf{S} \mathbf{N}_u d\Omega = \mathbf{G}^{-1} \mathbf{A} \quad (10) \end{aligned}$$

Enforcing the stationarity of (9) yields to

$$\partial_{\hat{\mathbf{u}}} \Pi_e^h = \mathbf{0} \implies \mathbf{C}^T \hat{\boldsymbol{\sigma}} = \mathbf{F}_e \quad (11)$$

$$\partial_{\hat{\boldsymbol{\varepsilon}}} \Pi_e^h = \mathbf{0} \implies \hat{\boldsymbol{\sigma}} = \mathbf{E} \hat{\boldsymbol{\varepsilon}} \quad (12)$$

$$\partial_{\hat{\boldsymbol{\sigma}}} \Pi_e^h = \mathbf{0} \implies \hat{\boldsymbol{\varepsilon}} = \mathbf{C} \hat{\mathbf{u}} \quad (13)$$

which can be combined into

$$\mathbf{K}_e^c \hat{\mathbf{u}} = \mathbf{F}_e \quad (14)$$

where $\mathbf{K}_e^c = \mathbf{C}^T \mathbf{E} \mathbf{C}$ is the positive-semi definite local stiffness matrix consistent with the strain and displacement models. Positive definiteness is achieved if:

- the 6 rigid body motions (RBM) are constrained (through standard FEM assembly and enforcement of kinematic Dirichlet conditions);
- \mathbf{C} has rank equal to the number of parameters describing the displacement field diminished by the RBM, $n_u - 6$.

The last condition cannot be satisfied if the strain field described by n_ε parameters is not rich enough, namely if $n_\varepsilon < n_u - 6$ an additional fictitious stiffness, the stabilizing matrix \mathbf{K}_e^s must be implemented to suppress the rise of spurious hourglass modes. To build \mathbf{K}_e^s one can add to the functional (6) an extra elastic potential through a fictitious material stiffness \mathbf{D}_H

$$\frac{1}{2} \hat{\mathbf{u}}_H^T \left(\int_{\Omega_e} \mathbf{B}^T \mathbf{D}_H \mathbf{B} d\Omega \right) \hat{\mathbf{u}}_H \quad (15)$$

where \mathbf{B} is the standard FEM compatibility matrix and $\hat{\mathbf{u}}_H$ are the hourglass displacement parameters. Splitting $\hat{\mathbf{u}}$ in the component generating deformation and RBM from the first natural parameters $\hat{\mathbf{p}}_{D+R}$ and the component producing hourglass modes from the second natural parameters $\hat{\mathbf{p}}_H$

$$\hat{\mathbf{u}} = \hat{\mathbf{u}}_{D+R} + \hat{\mathbf{u}}_H = [\mathbf{T}_{D+R} \ \mathbf{T}_H] \begin{Bmatrix} \hat{\mathbf{p}}_{D+R} \\ \hat{\mathbf{p}}_H \end{Bmatrix} \quad (16)$$

and exploiting the orthogonality between these two

$$(\hat{\mathbf{u}}_{D+R})^T \hat{\mathbf{u}}_H = \mathbf{0} \implies (\mathbf{T}_{D+R})^T \mathbf{T}_H = \mathbf{0} \quad (17)$$

leads to

$$\begin{aligned} \hat{\mathbf{u}}_H &= \mathbf{T}_H \hat{\mathbf{p}}_H = \left[\mathbf{I} + \right. \\ &\quad \left. -\mathbf{T}_{D+R} [(\mathbf{T}_{D+R})^T \mathbf{T}_{D+R}]^{-1} (\mathbf{T}_{D+R})^T \right] \hat{\mathbf{u}} = \\ &= \mathbf{H} \hat{\mathbf{u}} \end{aligned} \quad (18)$$

Enforcing the stationarity of the modified Hu-Washizu functional after the addition of (15) yields to

$$(\mathbf{K}_e^c + \mathbf{K}_e^s) \hat{\mathbf{u}} = \mathbf{F}_e \quad (19)$$

where \mathbf{K}_e^s is the *local stabilizing stiffness matrix*

$$\mathbf{K}_e^s = \mathbf{H}^T \left(\int_{\Omega_e} \mathbf{B}^T \mathbf{D}_H \mathbf{B} d\Omega \right) \mathbf{H} \approx \quad (20)$$

$$\approx \frac{1}{2} \text{tr}(\mathbf{K}_e^c) \mathbf{H}^T \mathbf{H} = \frac{1}{2} \text{tr}(\mathbf{K}_e^c) \mathbf{H} \quad (21)$$

where *scalar based stabilization* is adopted to approximate the integral in round brackets and the identity $\mathbf{H}^T \mathbf{H} = \mathbf{H}$ is exploited ([1]).

The assembly, solution and strain and stress recovery follow naturally.

2. Virtual Element Method

From the Hu-Washizu mixed finite element formulation, the k^{th} order VEM is derived starting from the definition of the approximate fields. The $[3 \times n_u]$ local displacement field \mathbf{N}_u

$$\mathbf{N}_u = \begin{bmatrix} N_1^u & 0 & 0 & \dots & N_{N_{DOF}}^u & 0 & 0 \\ 0 & N_1^u & 0 & \dots & 0 & N_{N_{DOF}}^u & 0 \\ 0 & 0 & N_1^u & \dots & 0 & 0 & N_{N_{DOF}}^u \end{bmatrix}$$

is *virtual*, meaning each shape function N_j^u :

- is a polynomial of degree k on each edge E of the polyhedron P ($N_j^u|_E \in \mathcal{P}_k(E)$)
- is globally continuous on the boundary ∂P ($N_j^u|_{\partial P} \in C^0(\partial P)$)
- its Laplacian is a polynomial of degree $k-2$ in P ($\Delta N_j^u \in \mathcal{P}_{k-2}(P)$)
- on every face F of P its Laplacian is a polynomial of degree k ($\Delta N_j^u|_F \in \mathcal{P}_k(F)$)
- on every face F of P , for any scaled monomial of degree $|\alpha| = k-1, k$, it holds

$$\int_F N_j^u|_F m_\alpha d\Sigma = \int_F [\Pi_{F,k}^\nabla N_j^u|_F] m_\alpha d\Sigma \quad (22)$$

where $\Pi_{F,k}^\nabla$ is the well known (in VEM literature) *projection operator*.

The degrees of freedom (DOFs) uniquely identifying an element N_j^u are

- the values of N_j^u at each vertex V of P (vertex-type)
- for each edge E of P , the values of N_j^u at the $k-1$ internal points of the $k+1$ Gauss-Lobatto quadrature rule (edge-type)
- for each face F of P , the $n_{k-2} = \dim([\mathcal{P}_{k-2}]^2)$ moments up to order $k-2$ of N_j^u over F (face-type)

$$\frac{1}{|F|} \int_F N_j^u|_F m_\alpha d\Sigma, \quad \alpha = 1, \dots, n_{k-2} \quad (23)$$

- the $\nu_{k-2} = \dim([\mathcal{P}_{k-2}]^3)$ moments up to order $k-2$ of N_j^u over P (polyhedron-type)

$$\frac{1}{|P|} \int_P N_j^u \mu_\alpha d\Omega, \quad \alpha = 1, \dots, \nu_{k-2} \quad (24)$$

One could retrieve the explicit form of N_j^u after solving a PDE, but this is never required as the DOFs are carefully selected so that they allow to build the VEM matrices. The $[6 \times n_\varepsilon]$ local strain field \mathbf{N}_ε is polynomial, as it contains the scaled monomials representing the projections of

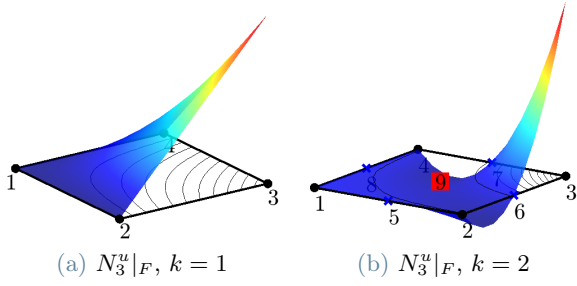


Figure 2: Shape function restricted on a face.

the strain field derived from the virtual displacements.

$$\mathbf{N}_\varepsilon = \begin{bmatrix} \mathbf{1}_{6 \times 6} & \xi \mathbf{I}_{6 \times 6} & \eta \mathbf{I}_{6 \times 6} & \cdots & \mu_{\nu_{k-1}} \mathbf{I}_{6 \times 6} \end{bmatrix}$$

Hence, matrices \mathbf{G} and \mathbf{E} are computable, and integrating by parts \mathbf{A} yields to

$$\mathbf{A} = \underbrace{\sum_{F \in \partial P} \left[\int_F (\mathbb{N}_F \mathbf{N}_\varepsilon)^T \mathbf{N}_u d\Sigma \right]}_{\mathbf{A}_1} + \quad (25)$$

$$- \underbrace{\int_P (\mathbf{S}^T \mathbf{N}_\varepsilon)^T \mathbf{N}_u d\Omega}_{\mathbf{A}_2} \quad (26)$$

where \mathbb{N}_F is the matrix of the outward normal unit vector of ∂P in F . \mathbf{A}_2 (appearing only for $k \geq 2$) is computable exploiting the internal moment polyhedron-type DOFs. For \mathbf{A}_1 one needs to address (22), after having computed first the projections $\Pi_{F,k}^\nabla$.

To construct \mathbf{H} , the only requirement is to build the matrix \mathbf{T}_{D+R} , gathering deformation and rigid body modes. Since these are captured by the $(k-1)$ -degree polynomial strain field, the displacement field purified from hourglass modes must be a k -degree polynomial.

$$\mathbf{u}_{D+R}(\boldsymbol{\xi}) = \mathbf{N}_k(\boldsymbol{\xi}) \hat{\mathbf{p}}_{D+R}$$

where

$$\mathbf{N}_k = \begin{bmatrix} \mathbf{1}_{3 \times 3} & \xi \mathbf{I}_{3 \times 3} & \eta \mathbf{I}_{3 \times 3} & \cdots & \mu_{\nu_k} \mathbf{I}_{3 \times 3} \end{bmatrix}$$

and remembering (16), the following identity holds

$$\mathbf{N}_k(\boldsymbol{\xi}) \hat{\mathbf{p}}_{D+R} = \mathbf{N}_u(\boldsymbol{\xi}) \mathbf{T}_{D+R} \hat{\mathbf{p}}_{D+R} \quad (27)$$

which can be used to construct \mathbf{T}_{D+R} exploiting the Lagrangian interpolation property of the

shape functions N_j^u .

$$\mathbf{T}_{D+R} = \begin{bmatrix} \mathbf{I} & \xi_1 \mathbf{I} & \cdots & \mu_{\nu_{k1}} \mathbf{I} \\ \mathbf{I} & \xi_2 \mathbf{I} & \cdots & \mu_{\nu_{k2}} \mathbf{I} \\ \vdots & \vdots & \ddots & \vdots \\ f_F \mathbf{I} & f_F \xi \mathbf{I} & \cdots & f_F \mu_{\nu_k} \mathbf{I} \\ f_F \xi_f \mathbf{I} & f_F \xi_f \xi \mathbf{I} & \cdots & f_F \xi_f \mu_{\nu_k} \mathbf{I} \\ \vdots & \vdots & \ddots & \vdots \\ f_P \mathbf{I} & f_P \xi \mathbf{I} & \cdots & f_P \mu_{\nu_k} \mathbf{I} \\ f_P \xi \mathbf{I} & f_P \xi^2 \mathbf{I} & \cdots & f_P \xi \mu_{\nu_k} \mathbf{I} \\ \vdots & \vdots & \ddots & \vdots \end{bmatrix} \quad (28)$$

Finally, the part of the equivalent nodal forces vector generated from surface tractions \mathbf{F}_e^p can be found exploiting the projections $\Pi_{F,k}^\nabla N_j^u$ computed for the entries of \mathbf{A}_1 . The part \mathbf{F}_e^b generated by body forces \mathbf{b} can be computed differently according to the VEM order: if $k = 1$ body forces are uniformly distributed on the N_V nodes, if $k = 2$ they are projected onto the space $[\mathcal{P}_{k-2}]^3$, obtaining the coefficients $\hat{\mathbf{b}}_i^h$ of the scaled monomial μ_i .

$$k = 1 \implies \mathbf{F}_e^b = \frac{1}{N_V} \begin{Bmatrix} \int_P \mathbf{b} d\Omega \\ \vdots \\ \int_P \mathbf{b} d\Omega \end{Bmatrix} \quad (29)$$

$$k = 2 \implies \mathbf{F}_e^b = \frac{1}{N_V} \begin{Bmatrix} \mathbf{0} \\ \vdots \\ \hat{\mathbf{b}}_1^h \\ \vdots \\ \hat{\mathbf{b}}_{\nu_{k-2}}^h \end{Bmatrix} \quad (30)$$

3. Numerical tests of hourglass-stabilized VEM

The following problem is numerically solved with hourglass-stabilized $k = 1$ and $k = 2$ VEM

$$\begin{cases} -\mathbf{S}^T [\mathbf{D}(\mathbf{S}\mathbf{u})] = \mathbf{b} & \text{in } \Omega = [0, 1]^3 \\ \mathbf{u} = \mathbf{0} & \text{on } \partial\Omega \end{cases} \quad (31)$$

with trigonometric body forces $\mathbf{b}(\mathbf{x})$ so that

$$\mathbf{u}(\mathbf{x}) = C \sin(\pi x) \sin(\pi y) \sin(\pi z) \{1 \ 1 \ 1\}^T$$

with $C = 0.1$ being a constant. Six different meshes composed by the elements in Figure 3 are tested and h -convergence results are shown in Figures 4, 5.

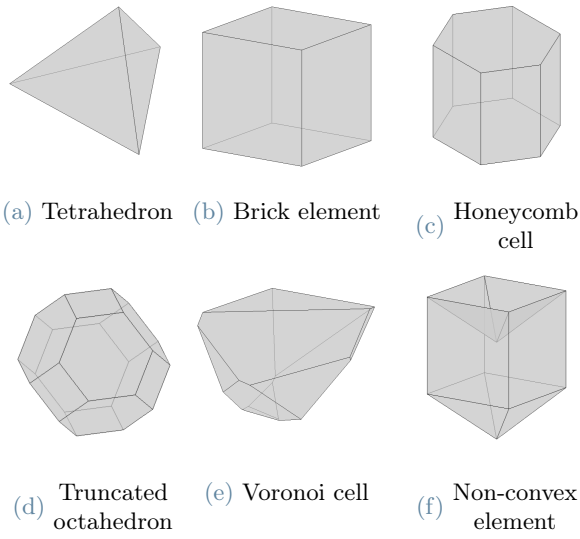


Figure 3: Polyhedral elements for the considered meshes.

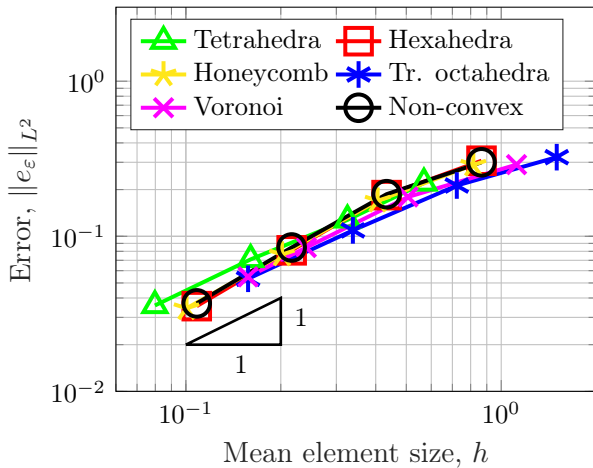


Figure 4: h -refinement convergence test, $k = 1$.

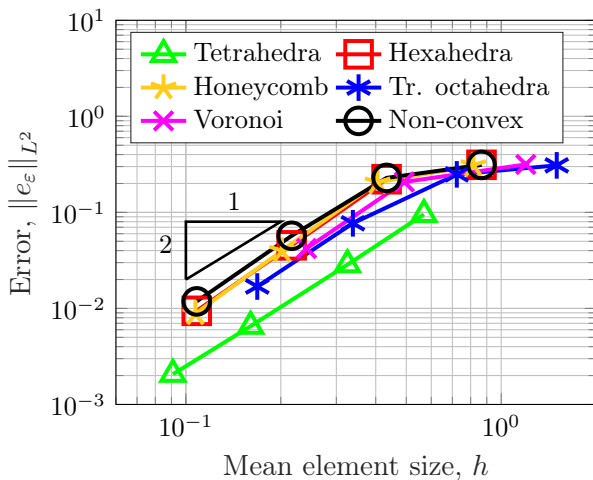


Figure 5: h -refinement convergence test, $k = 2$.

4. Δ VEM and self-stabilization

For virtual elements of order $k = 1$, if the faces of the polyhedra are triangles instead of general polygons, projecting the restrictions of the shape functions $N_j^u|_F$ over the faces is not necessary anymore as these become linear functions.

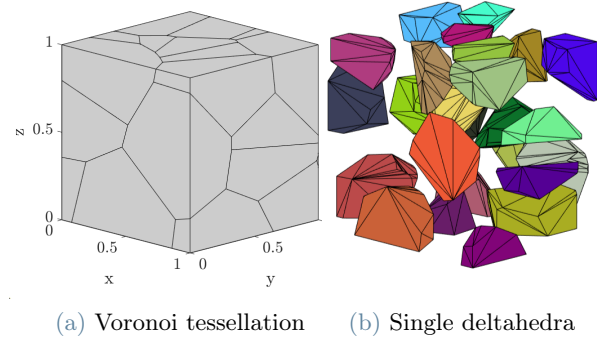


Figure 6: Deltahedral mesh (b) obtained by triangulating the faces of a Voronoi tessellation (a).

If the strain field is still constant over the element as with $k = 1$ VEM, computing the entries of matrix \mathbf{A}_1 greatly simplifies

$$\int_F n_i N_j^u d\Sigma = \begin{cases} n_i \frac{|F|}{3} & \text{if vertex } j \text{ is on face } F \\ 0 & \text{otherwise} \end{cases}$$

To achieve self-stabilization ([3]), an enhanced strain formulation is adopted and applied to a *brick-type deltahedron*, starting from $k = 1$ VEM. Such element P enjoys:

- 24 vertex-type DOFs
- the fact that the restriction of the virtual displacement shape functions on the faces of the element is piecewise linear ($N_j^u|_F \in \mathcal{P}_k(F)$) and globally continuous ($N_j^u|_F \in C^0(\partial P)$)

Remembering the decomposition of matrix \mathbf{A} in (25), one should notice that \mathbf{A}_2 is computable only if internal moments DOFs are available or if the strain field is divergence-free ($\mathbf{S}^T \mathbf{N}_\varepsilon = \mathbf{0}$). Hence, a careful selection of such field must be envisaged to guarantee

- the correct rank of \mathbf{C} , $\text{rank}(\mathbf{C}) = n_u - 6$, which does not hold if $n_\varepsilon < n_u - 6$;
- computability of matrix \mathbf{A}_2 .

It was noted that a linear complete strain field with $n_\varepsilon = 24$ parameters and the introduction of three 0th order internal moments leads to $\text{rank}(\mathbf{C}) = 18 \neq n_u - 6 = 21$, having the number

of DOFs increased to 27. The largest divergence-free subspace of a linear strain field has $n_\varepsilon = 15$, which satisfy $n_\varepsilon < n_u - 6 = 18$, meaning stabilization would still be required. Therefore, the polynomial degree of the strain model has been further increased. Three divergence-free quadratic strain fields are proposed for a 8-nodes, 24-DOFs self-stabilized VE:

- 31 parameters, developed from a complete *Airy function* $\phi(\boldsymbol{\xi}) \in \mathcal{P}_4$ (VEM8SS31)
- 25 parameters, developed from the symmetric gradient of a displacement field $\mathbf{u}(\boldsymbol{\xi}) \in [\mathcal{P}_3]^3$ (VEM8SS25)
- 18 parameters, developed from a linear field with the addition of three quadratic parameters (VEM8SS18).

Proving that the stiffness matrices \mathbf{K}_e generated by the above models exhibit the correct rank deficiency is an extremely difficult task, hence a numerical optimization has been performed to find the configuration of the elements which lead to the closest-to-zero 7th smallest eigenvalue of \mathbf{K}_e , λ_7^{\min} , and compared with the largest eigenvalue λ_{\max} . The ratios between these were found to be $\frac{\lambda_7^{\min}}{\lambda_{\max}} < 8e-5$, partially validating the elements, but improvements of the optimization can be sought in a more sophisticated search, implementing a refined definition of the constraints and the multi-start approach.

5. Numerical tests of self-stabilized VEM

Diverse convergence tests with trigonometric and polynomial known solution proved the robustness of the three proposed self-stabilized VE and their superior accuracy against locking phenomena w.r.t. standard VEM. Results for problem (31) are shown here in Figure 7, and compared to standard $k = 1, 2$ VEM and Δ VEM.

6. Conclusions

A version of the VEM for three-dimensional elastostatics has been comprehensively presented, starting from a mixed variational formulation based on the three-field Hu-Washizu functional. The robustness of the solver was assessed through a MATLAB[®] implementation developed from scratch, emphasizing the strengths of the VEM with respect to standard FEM (distortion insensitivity, non-convexity of

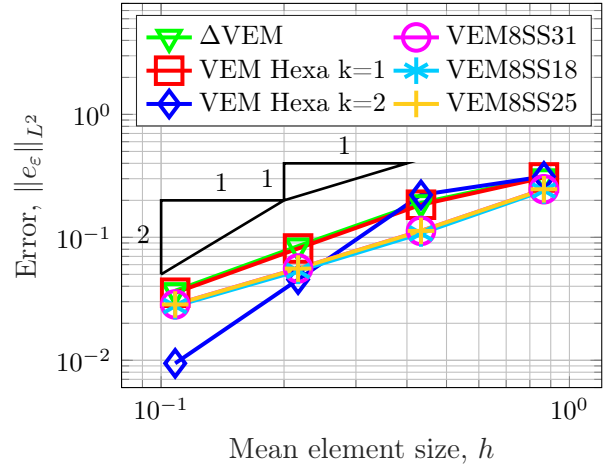


Figure 7: h -refinement test, SSVEM.

mesh). Subsequently, polyhedra with only triangular faces (*deltahedra*, hence Δ VEM) were introduced to ease the VE projection operation on their boundary and three enhanced strain self-stabilized VEM formulations have been proposed and successfully tested. Starting from a $k = 1$ 8-nodes brick-type Δ VEM, it has been shown how a linear strain field would still require stabilization, while 31-, 25- and 18-strain-parameters 8-nodes 24-DOFs self-stabilized VEM were developed and tested through an eigenvalue optimization and h -refinements, showing an increased accuracy and better locking behavior w.r.t standard VEM.

References

- [1] Edoardo Artioli, L Beirão da Veiga, Carlo Lovadina, and Elio Sacco. Arbitrary order 2d virtual elements for polygonal meshes: part i, elastic problem. *Computational Mechanics*, 60:355–377, 2017.
- [2] L Beirão da Veiga, Franco Brezzi, Luisa Donatella Marini, and Alessandro Russo. The hitchhiker’s guide to the virtual element method. *Mathematical models and methods in applied sciences*, 24(08):1541–1573, 2014.
- [3] Andrea Lamperti, Massimiliano Cremonesi, Umberto Perego, Alessandro Russo, and Carlo Lovadina. A hu–washizu variational approach to self-stabilized virtual elements: 2d linear elastostatics. *Computational Mechanics*, 71(5):935–955, 2023.